Colloidal glasses

2008 J. Phys.: Condens. Matter 20 494202

(http://iopscience.iop.org/0953-8984/20/49/494202)

IOP PUBLISHING JOURNAL OF PHYSICS: CONDENSED MATTER

J. Phys.: Condens. Matter **20** (2008) 494202 (6pp) doi:10.1088/0953-8984/20/49/494202

Colloidal glasses

P N Pusey

SUPA, School of Physics and Astronomy, Edinburgh University, Mayfield Road, Edinburgh EH9 3JZ, UK

Received 13 August 2008
Published 12 November 2008
Online at stacks.iop.org/JPhysCM/20/494202

Abstract

At high enough concentrations, suspensions of microscopic particles in a liquid can form 'colloidal glasses'. These are metastable amorphous solids in which the particles are trapped by their neighbours but still have some freedom for local Brownian motions. Typically they are 'soft' solids which yield and flow under applied stresses. This article describes some experimental studies of colloidal glasses of spherical particles. The Brownian dynamics of quiescent, unstressed, systems can be measured using dynamic light scattering. Various rheological techniques give information on mechanical properties and the mechanisms of yielding. Emphasis is on exploring the striking differences between glasses formed by particles with purely repulsive interactions and those with additional short-ranged attractions.

1. Introduction

Colloidal glasses are concentrated suspensions of microscopic particles in a liquid in which the particles' motions are constrained; they retain some freedom for local Brownian motions but are unable to diffuse over large distances. Because of this localization, colloidal glasses at rest are amorphous solids. However, they are typically soft solids, deforming elastically under small applied stresses, but yielding and flowing when stressed more strongly. A nice example is toothpaste which flows from the tube but sits as a solid piece of material on the brush.

This article will compare and contrast the behaviour of two types of colloidal glass. In 'repulsive' glasses, the localization of the particles results simply from crowding or 'jamming': at high concentrations, each particle is surrounded by a 'cage' of neighbours, able to 'rattle' within its cage, but unable to escape. In 'attractive' glasses, attractions between the particles cause bonded networks: the particles can rattle a little by stretching the bonds, but, with strong enough attraction, the bonds are effectively permanent, preventing any large-scale motion. Both the quiescent Brownian dynamics of the unstressed materials, studied by dynamic light scattering, and the mechanisms by which they yield and flow when stressed in a rheometer will be described.

This is a story that spans more than 20 years. It starts with early studies of repulsive 'hard-sphere' glasses in the 1980s, covers the quiescent behaviour of attractive glasses starting around 2000, and comes up-to-date with recent rheological studies of both systems. As this is the report of a conference lecture, I will be economical with details. These, including more complete bibliography, can be found in the papers cited.

2. Repulsive 'hard-sphere' glasses

2.1. Phase behaviour

The equilibrium phase behaviour of assemblies of equal-sized hard spheres was established many years ago by computer simulation (Alder and Wainwright 1957, Hoover and Ree 1968). It is determined by just one parameter, the fraction of the volume of the sample that is occupied by the particles: the volume fraction, ϕ. Up to a volume fraction $\phi = 0.494$, the equilibrium state is a fluid with short-ranged order in which the particles can diffuse throughout the sample. For $\phi > 0.545$, the state is a crystal. At $\phi = 0.545$ the crystal is quite loose, with significant motions of the particles around their lattice sites; it can be compressed up to touching close packing at $\phi = 0.74$. For $0.494 < \phi < 0.545$, fluid and crystal coexist.

Colloidal particles can be made whose interaction closely approximates that of hard spheres. Suspensions of such particles, in which Brownian motion allows thermodynamic equilibrium to be reached, can therefore be used to test the predictions of these computer simulations. Pusey and van Megen (1986) used particles consisting of solid amorphous cores of poly-methylmethacrylate (PMMA) whose surfaces were grafted with thin layers of another, flexible, polymer. When two such particles approach each other, compression of their polymer layers results in a steep, nearly hard-sphere, repulsion. The mean radius of the particles was $R = 320$ nm and the polydispersity (standard deviation of the size distribution divided by its mean) was about 0.05. They were suspended in a mixture of organic liquids chosen to roughly match the refractive index of the particles, thus rendering the samples nearly transparent.

Samples were mixed thoroughly and left to stand undisturbed. After one day they showed much of the predicted equilibrium phase behaviour, including fluid, fluid–crystal coexistence, and crystal. However, around $\phi = 0.58$, a striking change in the nature of the crystallization was observed, from a large number of very small homogeneously nucleated crystals to a much smaller number of large irregular crystallites, apparently nucleated heterogeneously. At slightly higher concentrations, $\phi > 0.58$, no crystallization was observed and the samples remained amorphous, even though the predicted equilibrium state was a crystal. This observation was interpreted as a glass transition and the high-concentration amorphous samples were identified as colloidal glasses.

2.2. Microscopic dynamics by DLS

The microscopic Brownian motions underlying this glass transition can be studied by dynamic light scattering (DLS). DLS measures the normalized intermediate scattering function

$$f(q,\tau) \equiv \frac{F(q,\tau)}{F(q,0)}$$

where the intermediate scattering function

$$F(q,\tau) \equiv \left\langle \frac{1}{\sqrt{N}} \sum_{j=1}^{N} \exp(\mathbf{i}\boldsymbol{q}\cdot\boldsymbol{r}_j(0)) \times \frac{1}{\sqrt{N}} \sum_{k=1}^{N} \exp(-\mathbf{i}\boldsymbol{q}\cdot\boldsymbol{r}_k(\tau)) \right\rangle$$

can be interpreted as the time-correlation function of the spatial Fourier component of density having wavevector $\boldsymbol{q}$ (the scattering vector). Here N is the number of particles, $\boldsymbol{r}_j(t)$ is the position of particle j at time t and τ is the correlation delay time. Thus DLS measures the stochastic dynamics of 'density waves' of wavelength $2\pi/q$ (e.g. Pusey 2002). While $f(q,\tau)$ is strictly a collective property, depending on the correlated positions of different particles at different times, it is frequently adequate and instructive to discuss DLS data in terms of the motions of single particles.

The first study of the hard-sphere colloidal glass transition by DLS (Pusey and van Megen 1987) was followed by more detailed investigations (e.g. van Megen and Underwood 1994). Experiments were performed on samples, similar to those described above, immediately after they had been thoroughly mixed and before any crystallization had taken place. They were thus in fluid, metastable fluid, or glassy states.

The intermediate scattering functions $f(q,\tau)$ of concentrated suspensions consist of a fast decay, sometimes called β-relaxation, followed the slower α-relaxation (van Megen and Underwood 1994). The β-relaxation is associated with the local Brownian motions, or rattling, of the particles within their cages, whereas the longer-time α-relaxation reflects escape from the cages and the diffusion of particles over distances comparable to or large compared to their size. As the particle concentration was increased from below $\phi = 0.494$ to above $\phi = 0.58$, it was found that the β-relaxations slowed down only slightly, implying that, even at high concentrations, the particles retained freedom for local rattling. The α-relaxations, however, exhibited a dramatic slowing. Going from $\phi = 0.494$ (the highest-concentration equilibrium fluid) to $\phi \approx 0.56$, a slowing down of about two decades in time was found. Going from $\phi \approx 0.56$ to just $\phi \approx 0.57$ gave another two decades of slowing. And at $\phi \approx 0.58$, $f(q,\tau)$ hardly decayed at all in the α-relaxation regime, reaching a nearly time-independent plateau. In terms of the cage picture, these observations imply an increasing tightening of the cages as the concentration is increased, so that particles become trapped for longer and longer times before escaping into new cages. At $\phi \approx 0.58$, particles become permanently trapped on the timescale of the experiment. Associated with this trapping is the partial 'freezing-in' of density fluctuations on all length scales.

A striking feature of these experiments was the coincidence, at $\phi \approx 0.58$, of the macroscopic indication of a glass transition, the suppression of crystallization, and its microscopic counterpart, the freezing-in of density fluctuations or 'structural arrest'.

This work on colloidal glasses was motivated partly by an earlier prediction, by mode-coupling theory (MCT), of a glass transition in an assembly of hard spheres (Bengtzelius *et al* 1984). MCT takes the dynamical equations describing the system—Newton's equations for atoms or Langevin's equations for colloids—and applies the well-defined 'mode-coupling' approximation. This approximation is uncontrolled in the sense that it is difficult to estimate the importance of the terms omitted in the development. Nevertheless MCT is still the only theory of the glass transition able to give detailed predictions for the behaviour of quantities such as intermediate scattering functions (e.g. Götze and Sjögren 1992). After allowance is made for the different values for the concentration of the glass transition predicted by theory and observed experimentally, good agreement is found between the intermediate scattering functions measured on colloidal systems and those predicted by MCT (van Megen and Underwood 1994).

3. Attractive glasses

Despite this good agreement between experiment and theory, mode-coupling theory remained somewhat controversial, partly for the perceived lack of a clear underlying 'physical picture'. A major boost for MCT came when Fabbian *et al* (1999) and Bergenholtz and Fuchs (1999) considered the effect of adding a short-ranged attraction to the hard-sphere repulsion between particles. These authors predicted, via MCT, a rich new scenario of glass transitions involving a new type of 'attractive' glass. A specific prediction, relevant here, was that of a 're-entrant' transition over a significant range of particle concentrations: as the strength of the attraction was increased from zero, an initially hard-sphere glass would first melt to a metastable fluid (which could crystallize), then re-freeze into the new attractive glass. In the attractive glass, essentially a concentrated network of particles bonded by the attraction, the local rattling of the particles was predicted to be much more restricted spatially than in repulsive glasses.

Around 2000 we set out to test these predictions using colloidal particles with an attraction induced by the depletion

effect of added, non-adsorbing, polymer molecules (Pham *et al* 2002, 2004b). When, in a polymer solution, two colloidal particles approach each other so that their surfaces are separated by less than the diameter of the polymer molecules, polymer is excluded from a 'depletion region' between the particles. As a result, the polymer molecules are no longer distributed isotropically around each particle. This anisotropy causes unbalanced osmotic pressures which push the two particles towards each other. The effect can be described by an effective attractive interparticle interaction potential. A nice feature of this depletion attraction is that both its range and its strength can be easily controlled experimentally. The relative range is determined by the relative size of the polymer molecules and the particles, and the strength is determined by the concentration of added polymer (which controls the osmotic pressure).

We used PMMA particles, similar to those described above, and polystyrene polymer (Pham *et al* 2002, 2004b). The particle radius was 202 nm (polydispersity $\sim$ 0.07) and the radius of gyration of the polymer was 17.8 nm, giving a relative attraction range of $\sim$0.09. Here MCT predicts the re-entrant behaviour described above. Samples were prepared at a colloid volume fraction of $\phi \approx 0.60$ with increasing amounts of polymer and were thoroughly mixed. Direct observation verified, qualitatively, the MCT predictions. For little or no added polymer, the samples did not crystallize, presumably remaining as repulsive glasses. With a moderate amount of polymer, crystallization was observed after a day or two. With a lot of polymer, giving a strong interparticle attraction, crystallization was again suppressed—presumably the attractive glasses.

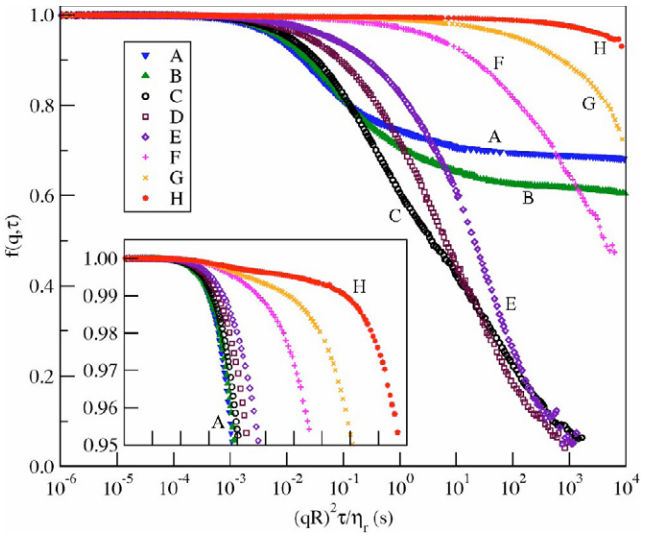

Figure 1. Intermediate scattering functions versus scaled time for samples of PMMA colloids with added polystyrene polymer at size ratio $\sim$0.09. Sample A is a hard-sphere glass with no added polymer; polymer concentration increases from B to H, the latter being the strongest attractive glass. The inset shows the same plots on an expanded vertical axis. The measurements were made at scattering vector $qR = 1.5$, well below the main peaks in the static structure factors. Time is scaled by $(qR)^2/\eta_r$, where η_r is the viscosity of the polymer solution relative to that of the solvent, thus removing the direct effect of the polymer on the dynamics. Real time ranges from about one half of scaled time for sample A to about four times scaled time for sample H. (From Pham *et al* 2004b. Copyright 2004, by the American Physical Society.)

(This figure is in colour only in the electronic version)

3.1. Dynamic light scattering

As with the pure repulsive glasses, more detailed information was obtained by DLS studies of the microscopic dynamics (Pham *et al* 2004b). In these measurements, improvements of the light scattering technique were employed to provide high-quality data over many decades of delay time (e.g. figure 1). Multiple scattering from the slightly turbid samples was suppressed by the two-colour DLS method (e.g. Segrè *et al* 1995); and efficient ensemble averaging over slow or arrested fluctuations was achieved with an 'echo' technique (Pham *et al* 2004a).

Figure 1 shows a good example of the DLS data. Sample A was a pure hard-sphere glass (no added polymer). After the initial β-relaxation, reflecting rattling in the cage, the intermediate scattering function reaches a plateau at $f(q,\tau) \approx 0.70$ associated with freezing-in of density fluctuations and the suppression of long-distance diffusion. Sample B, with a small amount of polymer, shows similar behaviour. By contrast, nearly complete decay of $f(q,\tau)$ was found for samples C, D and E, those which showed crystallization when observed directly. Then, with more polymer added, samples F, G and H, the (short-time) β-decay of $f(q,\tau)$ becomes strongly suppressed, though the inset to figure 1 shows that a weak decay, of amplitude less than 1% remains. For sample H, with the highest concentration of polymer, $f(q,\tau)$ decays by only 5% over about 10^4 s (nearly 3 h)—this is the strong attractive glass. (Note that if the sample were completely rigid, with microscopic motion totally suppressed, $f(q,\tau)$ would be equal to 1 at all times.)

A qualitative interpretation of these observations is the following. In the pure hard-sphere glass, sample A, the relatively large amplitude of the β-decay implies significant freedom for local particle motions and the nearly flat plateau implies permanent caging. The slightly lower plateau for sample B indicates slightly looser cages. The complete decay of $f(q,\tau)$ for samples C, D and E reflects complete relaxation of density fluctuations and the existence of large-scale diffusion, allowing crystallization. Here, the weak depletion attraction imposed by a moderate concentration of polymer apparently causes transient clustering of the particles and the opening of 'holes' in the cages allowing particles to escape. Finally, with more polymer and strong attraction, samples F, G and H, the particle clusters become long-lived. Although holes in the cages still exist, each particle is tightly bonded to its neighbours. Nevertheless, limited rattling of the particles, by stretching the bonds, still remains, as indicated by the small-amplitude β-decays seen in the inset to figure 1.

More extensive DLS data are shown in Pham *et al* (2004b). There we also describe how measurements of static structure factors fit the simple picture given above. With increasing polymer concentration, the main structure factor peak moves to larger scattering vector, implying smaller particle separations,

and reduces in amplitude, implying increased heterogeneity in the samples. This meso-scale heterogeneity also leads to a large increase in the magnitude of the structure factor at small scattering vectors.

4. Rheology: elasticity, yielding and flow

As described above, the existence of non-decaying plateaux in the intermediate scattering functions of colloidal glasses implies that the particles are localized; this, in turn, implies that the samples are solid. Yet we know that the samples can easily be 'melted' to metastable liquids by shaking or tumbling. Thus we can ask two questions: are colloidal glasses truly solid; and, if so, how do they yield and flow under the application of stress?

Over the past few years we have undertaken a detailed rheological study of repulsive and attractive colloidal glasses and the transition between them. This work is summarized in Pham *et al* (2008), where we describe the results of a number of rheological 'tests', including oscillatory shear, step strain, step stress, and steady shear flow experiments. In the limited space available here we consider just two of these measurements—small-amplitude oscillatory shear and strain recovery following step stress—which illustrate striking differences in the behaviours of the two types of glass.

As in the DLS experiments, we used PMMA particles with a depletion attraction induced by polystyrene polymer at size ratio about 0.08. The particles were smaller, radius 130 nm (cf 202 nm for DLS), and more polydisperse, ∼0.20 (cf 0.07). This larger polydispersity prevented crystallization. Here we describe experiments made on samples with a colloid volume fraction of ∼0.60 and polymer concentration increasing from zero, the hard-sphere glass, to a value large enough to form the attractive glass.

4.1. Oscillatory shear

Several types of rheological measurement can be used to address the first question: are colloidal glasses solid? A simple one is to apply an oscillatory strain to the sample with amplitude small enough, ∼1%, that the response is linear. One measures the magnitude and phase of the resulting stress on the sample. The in-phase component of the stress gives the (elastic) storage or shear modulus G' of the sample, whereas the out-of-phase component gives the viscous or loss modulus G''. One criterion for solidity is that a material's storage modulus should be greater than its loss modulus.

Our measurements showed that, over a range of frequency, both the hard-sphere and attractive glasses had storage moduli much larger than their loss moduli, indicating solidity (Pham *et al* 2008). At a frequency of 1 rad s^{-1}, the actual values of storage modulus were $G' \sim 60$ Pa for the hard-sphere glass and $G' \sim 500$ Pa for the attractive glass, showing that bonding greatly strengthens the material.

4.2. Step stress

Asked to decide whether material in a container is liquid or solid, most people would immediately poke it with a finger and observe the resulting behaviour: flow, elastic deformation and recovery, or permanent (plastic) deformation. The quantitative rheological equivalent of 'poke it and watch' is a step stress and recovery experiment. Here stress, usually a shear, is suddenly applied to a sample, is held at a constant magnitude for a period of time, and is then suddenly removed. Throughout this process, the strain of the sample is monitored. Subjected to this treatment, an ideal elastic solid would deform immediately, hold a constant strain, and recover its initial shape on removal of the stress. On the other hand a 'perfect' liquid would immediately start to flow, would increase its strain at a constant rate while the stress was applied, and cease flowing, retaining the accumulated strain, when the stress was removed.

A real soft material shows viscoelasticity, behaviour intermediate between these two extremes. At small values of the applied stress, elastic deformation and recovery is observed. At large enough applied stress, the sample flows. Nevertheless, some elastic recovery is frequently observed when the stress is removed. Real solid materials (even hard materials studied over a long enough time) also show the phenomenon of creep, the sub-linear increase of strain, $\gamma(t)$, with time during the application of a stress, i.e. $\gamma(t) \propto t^{\lambda}$, with $\lambda < 1$. Because of the complications introduced by creep, which is still not fully understood, we limit consideration here to the *recovery of strain after the stress is removed* (see Pham *et al* (2008) for more details of the full step stress results).

4.3. Recovery after step stress: hard-sphere glass

Figures 2(a) and (b) show the recovered strain versus time for hard-sphere and attractive glasses respectively (Pham *et al* 2008). In a series of measurements, the samples were subjected to a constant step stress, σ_c, for 1000 s, while monitoring the strain. The magnitude of σ_c was increased for each new measurement. The figures show the behaviour of the strain after the stress is removed.

The results for the hard-sphere glass, figure 2(a), show several features. (i) Immediately after the stress is removed there is a 'fast' recovery of strain, within 10^{-1} s. We found this fast recovery to have the same magnitude as the 'fast' deformation observed when the stress is first applied; we therefore attribute it to elastic deformation. (ii) The fast recovery is followed, over 10–1000 s, by a slower recovery of smaller but still significant magnitude. The origin of this slow recovery is not fully understood; possibly the underlying mechanisms are related to those of the creep phenomenon described above (Pham *et al* 2008). (iii) As the magnitude σ_c of the step stress is increased, the recovered strain first increases in proportion, then saturates at a value around 10%, independent of σ_c. Figure 2(c) plots the magnitudes of the fast recovered strain and the total recovered strain as functions of σ_c.

A possible explanation of some of these observations can be given in terms of the cage picture (Petekidis *et al* 2003, Pham *et al* 2008). When a small stress is applied to a hard-sphere glass it distorts macroscopically and, microscopically, each cage distorts accordingly while retaining its integrity (each particle retains the same topological neighbours). When

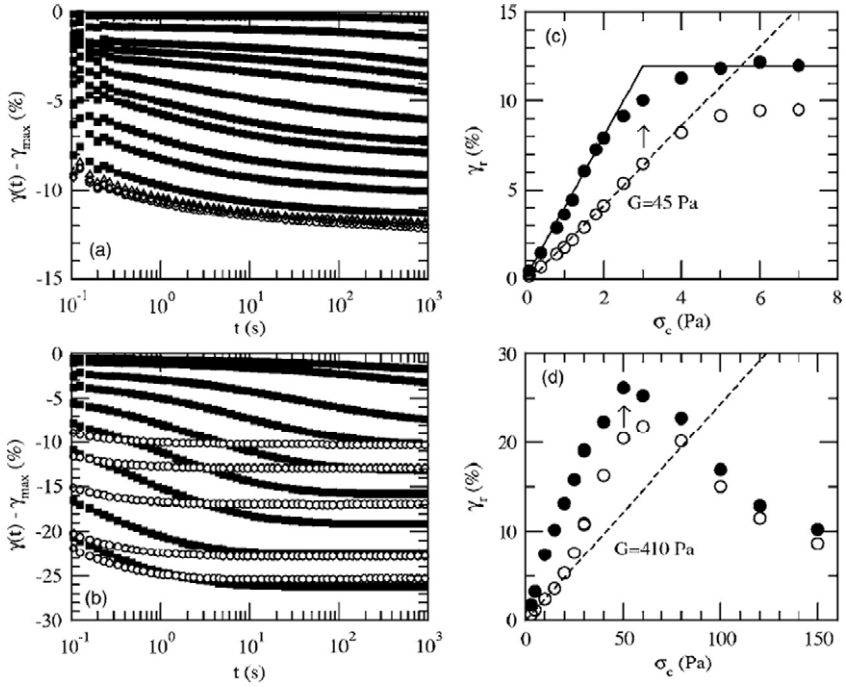

Figure 2. Strain recovery after removal of stress step for repulsive and attractive glasses. After the application of a step stress σ_c for 1000 s, the stress is removed. At this point the samples have accumulated a 'maximum' strain γ_{max}. The samples then recover a portion of this strain. Panels (a) and (c) show this recovery, plotted as $\gamma(t) - \gamma_{max}$ versus time. For the hard-sphere glass (a) the magnitude of the stress step σ_c increases from top to bottom; at the highest stresses a 'saturated' form is found for the recovery. For the attractive glass (b) σ_c increases from top to bottom at low stresses (closed symbols) and then from bottom to top at higher stresses (open symbols). The values of step stress used can be read from the x axes of panels (c) and (d). These show the magnitudes of the recovered strains γ_r as functions of the step stress, (c) hard-sphere glass, (d) attractive glass. Open symbols are the fast or 'instantaneous' recovered strains, estimated at $t = 0.1$ s from the data of (a) and (b). Closed symbols are the total recovered strains, measured at $t = 1000$ s. The dashed lines are linear fits to the fast recovered strains at small stresses. The solid lines in (c) are to guide the eye through the data in the low-stress, elastic, regime and the high-stress, saturated, regime. (From Pham *et al* 2008. Copyright 2008, The Society of Rheology.)

the applied stress is removed, the residual stress in the sample, which can be viewed as an anisotropic osmotic pressure, drives it back to its initial configuration; the cages recover their initial isotropy. However, larger stresses are able to break the particle cages, allowing the sample to flow. The fact that the recovered strain saturates at large stresses, figure 2(c), implies that, when the stress is removed from a flowing sample it finds itself with 'maximally distorted' cages which then relax to isotropy.

Interpreting the fast recovered strain at low stresses as an elastic distortion, we can calculate an elastic modulus from the data of figure 2(c). The value obtained, 45 Pa, compares reasonably well with that, 60 Pa, found in the oscillatory shear measurements described above. The value of the stress, indicated by the arrow in figure 2(c), at which the predominantly elastic behaviour (though complicated by creep) crosses over to the saturated, flow, behaviour, can be identified as the yield stress of the sample. Though not shown here (see Pham *et al* (2008)), this value, 3–4 Pa, agrees well with that where fully-developed flow, $\gamma(t) \propto t$, rather than creep, $\gamma(t) \propto t^{\lambda}$, with $\lambda < 1$, is first observed under stress.

4.4. Recovery after step stress: attractive glass

Compared to the hard-sphere glass, the attractive glass shows a much more complicated strain recovery behaviour, figure 2(b). Again, fast and slow recoveries are observed. But now the amplitudes of both recoveries are no longer monotonic functions of the applied stress. They show maximum values of more than 20%—much larger than for the hard-sphere glass, ∼10%—before reducing to about 10% at high stresses, figure 2(d).

We do not yet have a clear picture of the microscopic mechanisms underlying this complex behaviour. However a few points can be made. At low values of the applied stress σ_c, the fast recovered strain depends linearly on σ_c. This elastic behaviour can be attributed to stretching of the interparticle bonds, rather than to the cage elasticity mechanism described above for the hard-sphere glass. Again, the modulus, 410 Pa, obtained from these data compares quite well with that, 500 Pa, measured by oscillatory shear. At the largest values of the applied stress, $\sigma_c = 150$ Pa, where the sample flows, the recovery behaviour looks very similar to that of the hard-sphere glass (compare figures 2(a) and (b)). Here it seems that the interparticle attraction has little effect: particle bonds are broken by the flow as quickly as they are formed and, presumably, the microstructure of the flowing system is similar to that of hard spheres. As the stress is reduced and the rate of flow slows, bonding becomes more important, and the magnitude of the recovered strain increases. Here, perhaps, the residual structures immediately the stress is removed can be viewed as stretched clusters which then recover some isotropy.

Other measurements, such as (non-linear) oscillatory shear with increasing strain amplitude (Pham *et al* 2008), suggest a complicated, multi-stage, yielding behaviour for attractive glasses, involving first bond stretching and breaking at low stresses, followed by topological re-arrangement, or cage and cluster breaking, at higher stresses.

5. Summary and comments

We have described various properties of repulsive colloidal glasses, in which particles are caged by their neighbours, and attractive glasses, where interparticle bonding is the dominant influence. In both systems, structural arrest is indicated by nearly time-independent plateaux in the intermediate scattering functions measured by dynamic light scattering. The much higher plateau for the attractive glass implies a much more restricted local motion. Under stress, the repulsive glass shows relatively simple behaviour which can be interpreted as an elastic distortion of the particle cages at low stresses followed by cage breaking, leading to flow, at large stresses. The low-stress elastic behaviour of the attractive glass can be attributed to stretching of the interparticle bonds. Its yielding at larger stresses is a complicated process, involving both bond and cage breaking.

The experiments reported here, dynamic light scattering and rheology, measure average properties of the sample. However, glasses are known to be heterogeneous, exhibiting localized regions of dynamic activity: 'dynamic heterogeneities' in quiescent glasses (Kegel and van Blaaderen 2000, Weeks *et al* 2000) and the possibly related 'shear transformation zones' in stressed glasses (Schall *et al* 2007). It still remains to obtain a full picture of glass behaviour that reconciles the macroscopic average properties with the microscopic heterogeneity. In this connection, note that the microscopic mechanisms for yielding under stress—cage elasticity and breaking etc—suggested in the previous section are speculative. More study of the microscopic processes in colloidal glasses under stress, by confocal microscopy for example (e.g. Besseling *et al* 2007), is needed.

In common with most colloidal systems, the particles used in the work described here have a distribution of sizes (polydispersity). Although we have not emphasized it in this article, it is becoming increasingly apparent the even a small spread in particle size can strongly influence both crystallization and glass formation in colloidal systems (e.g. Schöpe *et al* 2007). In fact, there is evidence from computer simulation that an assembly of equal-sized hard spheres does not even show a glass transition (e.g. Rintoul and Torquato 1996). Recent calculation of the equilibrium phase diagram of polydisperse hard spheres shows a complicated structure for polydispersities greater than $\sim$0.05 which includes multiple crystal phases with different lattice parameters (Fasolo and Sollich 2004). Further work on the influence of polydispersity is necessary to obtain the full picture.

A second issue not discussed here is ageing, the slow change with time of properties of non-equilibrium systems after some initial preparation procedure. Again more work is needed; further discussion of and references to ageing are given in Pham *et al* (2008).

Acknowledgments

I am deeply indebted to the many colleagues and co-workers involved in the research described in this article. My early interest in colloidal systems would not have developed without the invaluable advice and help of Ron Ottewill. The work on hard-sphere glasses was the result of enjoyable collaborations with Bill van Megen. In Edinburgh, the experimental work on attractive glasses was co-supervised with Wilson Poon and Stefan Egelhaaf, and the particles were prepared by Andrew Schofield. Khoa Pham performed the DLS studies as a student and later, as a postdoctoral assistant, much of the rheological work. The rheology was started in Edinburgh by George Petekidis, and, after his return to Crete, continued with Dimitris Vlassopoulos. Mike Cates, Abdellatif Moussaïd, Antonio Puertas, Matthias Fuchs and Johan Bergenholtz all made important contributions to aspects of the research. The early work was supported by the UK Ministry of Defence, the work in Edinburgh by grants from the UK Engineering and Physical Sciences Research Council, the European Union, and Unilever Research.

References

Alder B J and Wainwright T E 1957 *J. Chem. Phys* **27** 1208
Bengtzelius U, Götze W and Sjölander A 1984 *J. Phys. C: Solid State Phys.* **17** 5915
Bergenholtz J and Fuchs M 1999 *Phys. Rev.* E **59** 5706
Besseling R, Weeks E R, Schofield A B and Poon W C K 2007 *Phys. Rev. Lett.* **99** 038301
Fabbian L, Götze W, Sciortino F, Tartaglia P and Thiery F 1999 *Phys. Rev.* E **59** R1347
Fasolo M and Sollich P 2004 *Phys. Rev.* E **70** 041410
Götze W and Sjögren L 1992 *Rep. Prog. Phys.* **55** 241
Hoover W G and Ree F H 1968 *J. Chem. Phys.* **49** 3609
Kegel W K and van Blaaderen A 2000 *Science* **287** 290
Petekidis G, Vlassopoulos D and Pusey P N 2003 *Faraday Discuss.* **123** 287
Pham K N, Egelhaaf S U, Moussaïd A and Pusey P N 2004a *Rev. Sci. Instrum.* **75** 2419
Pham K N, Egelhaaf S U, Pusey P N and Poon W C K 2004b *Phys. Rev.* E **69** 011503
Pham K N, Puertas A M, Bergenholtz J, Egelhaaf S U, Moussaïd A, Pusey P N, Schofield A B, Cates M E, Fuchs M and Poon W C K 2002 *Science* **296** 104
Pham K N, Petekidis G, Vlassopoulos D, Egelhaaf S U, Poon W C K and Pusey P N 2008 *J. Rheol.* **52** 649
Pusey P N 2002 *Neutrons, X-rays and Light: Scattering Methods Applied to Soft Condensed Matter* ed P Lindner and T Zemb (Amsterdam: North-Holland) p 203
Pusey P N and van Megen W 1986 *Nature* **320** 340
Pusey P N and van Megen W 1987 *Phys. Rev. Lett.* **59** 2083
Rintoul M D and Torquato S 1996 *Phys. Rev. Lett.* **77** 4198
Schall P, Weitz D A and Spaepen F 2007 *Science* **318** 1895
Schöpe H J, Bryant G and van Megen W 2007 *J. Chem. Phys.* **127** 084505
Segrè P N, van Megen W, Pusey P N, Schätzel K and Peters W 1995 *J. Mod. Opt.* **42** 1929
van Megen W and Underwood S M 1994 *Phys. Rev.* E **49** 4206
Weeks E R, Crocker J C, Levitt A C, Schofield A and Weitz D A 2000 *Science* **287** 627